Supplementary Information for "Accelerated identification of equilibrium structures of ternary compounds using machine learning potentials"

Sungwoo Kang,[1,2] Wonseok Jeong,[1,2] Changho Hong,[1] Seungwoo Hwang,[1] Youngchae Yoon,[1] and Seungwu Han[1]*

[1]Department of Materials Science and Engineering, Seoul National University, Seoul 08826, Korea [2]These authors contributed equally; Sungwoo Kang, Wonseok Jeong

Corresponding Author

*E-mail: hansw@snu.ac.kr

Effects of developed features

To explicitly show that the effect of MQ distance constraint in finding ground states, we replace the distance restraints in SPINNER with the conventional setting used in, for example, USPEX. Supplementary Figure 1 shows the energy distribution of the randomly-generated structures for Mg_2SiO_4, CdI_2O_6, and Sr_2P_7Br, in comparison with those generated by SPINNER employing the MQ distance constraint. It is seen that the MQ distance constraint produces low-energy structures far more frequently than the conventional setting. This means that the MQ distance constraint is highly effective in exploring the low-energy configurational space.

In Supplementary Figure 2, we compare the energy distribution obtained by the new crossover algorithm and those from the routine crossover algorithm. Although not as dramatic as the MQ distance constraints in the above (because the crossover maintains most of the bulk structures), the atomic-energy-based crossover algorithm is still effective in generating low-energy structures for the three test materials.

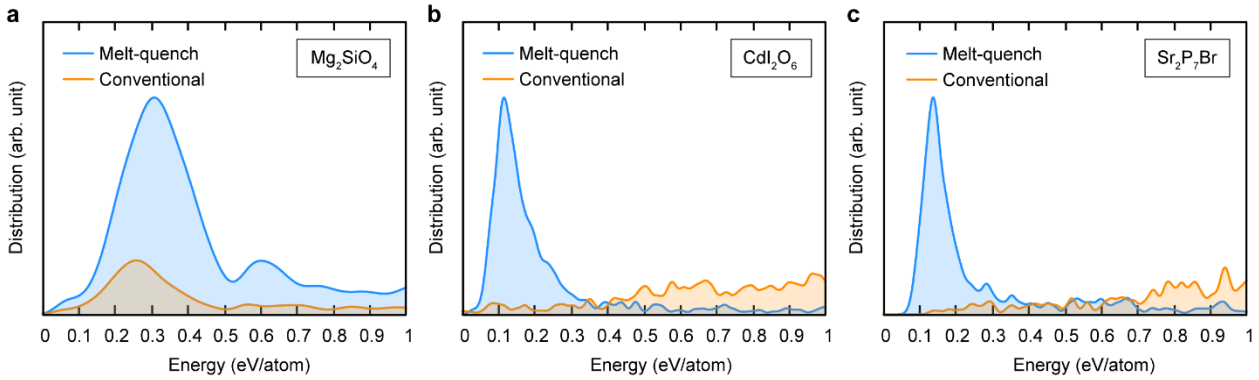

Supplementary Figure 1. The energy distribution of randomly generated and then relaxed structures using the distance constraint from melt-quench simulations (blue) and the loose distance constraint used in the USPEX code (orange) in the case of (a) Mg_2SiO_4, (b) CdI_2O_6, and (c) Sr_2P_7Br. The test structures are gathered after running the evolutionary algorithm for 200 generations under each condition.

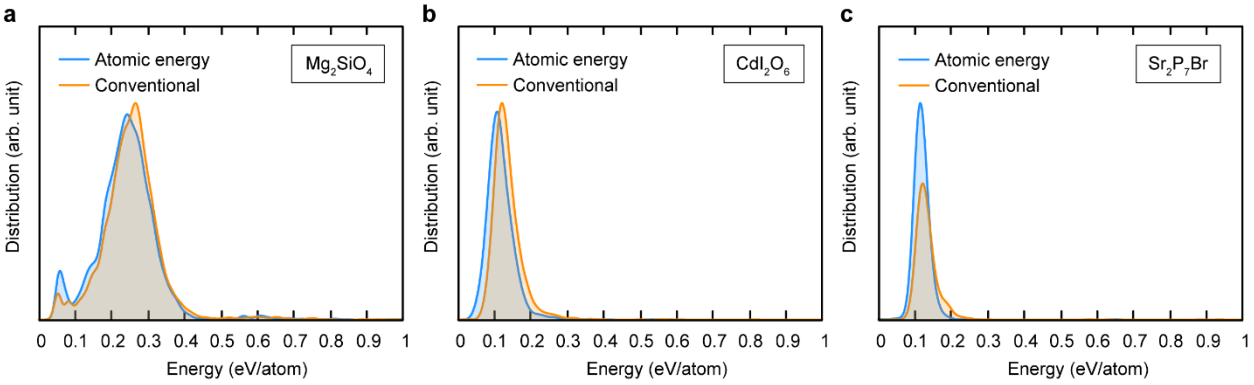

Supplementary Figure 2. Effect of the crossover algorithm. The energy distribution of structures generated by the atomic-energy-based crossover algorithm (blue) and the conventional crossover algorithm (orange), both of which are followed by structure relaxation in the case of (a) Mg_2SiO_4, (b) CdI_2O_6, and (c) Sr_2P_7Br. The test structures are gathered after running the evolutionary algorithm for 200 generations under each condition.

Supplementary Table 1. The table provides information and results on test compounds in Fig. 2a. The columns under ICSD are data on the equilibrium phase in the ICSD. Z and N_{at} are the numbers of formula units and atoms in the unit cell, respectively. Band gaps (E_g's) are calculated by one-shot hybrid functional calculations[1] and hull energies (E_{hull}'s) are cited from the Materials Project.[2] For the symbols under SPINNER, we refer to the main text. Under ΔE_{min} we write the energy difference between the most stable structure found by SPINNER within ICSD structure primitive cell size and the ICSD structure calculated by PBE functional. When needed, we additionally write the energy difference calculated by SCAN functional (marked by †), or by PBE when the spin-orbit coupling is considered (‡). Also, the numbers with the * mark indicate the energy difference between the most stable structure found within ICSD structure conventional cell size and the ICSD structure. The unit for E_{hull}, N_g, ΔE_0, $\Delta\bar{E}$, and ΔE_{min} are meV atom^{-1}.

Formula	ICSD						SPINNER			
	ID	Point group	Z	N_{at}	E_g (eV)	E_{hull}	N_g	ΔE_0	$\Delta\bar{E}$	ΔE_{min}
$PbOsO_3$	23444	$m\bar{3}m$	4	20	0	0	5	64.1	20.3	–15.6/ –4.0†/16.0‡
Tl_3PbCl_5	1262	4	4	36	6.0	9	11	3.8	5.9	–13.6/ 6.0†/ -0.2‡
Na_3PS_4	72860	$\bar{4}2m$	2	16	3.3	0	1	8.1	16.4	–9.1/22.3†
$RbInI_4$	36601	3m	6	36	3.5	0	990	2.9	11.9	–4.0/6.4†
$KAlCl_4$	1704	2	4	24	6.8	0	238	2.9	10.1	–2.7/9.5†

LiYSn	32041	6mm	8	24	0	0	13	3.3	12.6	–1.7/–2.0†
Na_3AsSe_3	50491	23	4	28	2.8	0	4004	1.4	7.3	0
AuOCl	8190	$\bar{3}$	6	18	2.3	0	723	22.0	20.1	0
Li_3AuO_3	15113	4/mmm	4	28	3.5	0	80	9.4	11.2	0
Na_3AuO_2	62066	4/mmm	4	24	3.1	0	344	2.5	3.1	0
KMo_3Se_3	603628	6/m	2	14	0	0	6	2.1	4.8	0
MgIrB	409979	622	6	18	0	0	46	1.1	4.3	0
$TlBO_2$	36404	4	8	32	3.8	0	5	0.1	4.7	0
$LiBaGe_2$	162583	mmm	4	16	0	0	17	9.1	13.6	0
Li_2BPt_3	156466	432	4	24	0	0	7	3.9	5.2	0
$LiBiO_3$	82277	mmm	8	40	1.2	0	3032	16.1	5.5	0
Sr_2P_7Br	429306	23	4	40	2.8	0	98	61.6	26.4	0
CaPdSi	69790	2/m	4	12	0	2	90	9.0	19.8	0
CdI_2O_6	1397	222	4	36	4.5	0	3030	9.0	19.8	0
Cs_2SbCl_6	49706	4/mmm	4	36	1.6	0	4	21.7	12.2	0
$LiWCl_6$	409938	3	4	32	0	12	739	8.1	14.4	0

$TlGaS_2$	157537	2/m	8	32	2.4	0	3	0.0	7.1	0
$TlGaSe_2$	1573	m	8	32	2.1	4	737	32.6	28.1	0
HfNbP	75009	mmm	4	12	0	0	32	3.7	2.6	0
Zr_2Pd_2In	107332	4/mmm	4	20	0	135	4	3.7	6.9	0
IrSbTe	640967	23	4	12	1.3	0	22	9.9	6.0	0
Li_2TeSe_3	415121	2/m	4	24	0.19	0	161	12.7	10.1	0
PbN_2O_6	174004	$m\bar{3}$	4	36	5.5	0	8	0.2	8.6	0
Na_3SbTe_3	75513	23	4	28	2.0	16	190	14.1	12.3	0
$TlSbO_3$	4123	$\bar{3}$m	4	20	3.3	135	27	5.2	7.5	0
Tl_3PS_4	201062	mmm	4	32	2.7	0	21	10.2	12.4	0
$BaIn_2Te_4$	41168	mmm	2	14	1.6	0	2802	10.1	16.9	0
Rb_2ZrTe_3	410735	2/m	4	24	0.14	0	25	44.4	8.6	0
Ag_2HgO_2	280333	422	4	20	1.3	0	321	22.1	16.3	0
RbAgO	40155	4/mmm	4	12	2.7	0	3577	19.8	9.7	0
$AsNb_3Te_3$	79934	6/m	2	14	0	0	408	48.2	35.5	0
$PbSnS_3$	23462	mmm	4	20	1.6	7	1528	35.1	16.0	0

$CaPS_3$	405192	2/m	4	20	4.1	0	131	4.9	11.9	0
$HfSiO_4$	31177	4/mmm	2	12	7.0	0	35	14.9	27.2	0
$NaScS_2$	644971	$\bar{3}$m	1	4	2.7	0	68	5.0	13.7	0
$MgTa_2O_6$	202688	4/mmm	2	18	4.2	0	9	2.4	7.3	0
Mg_2SiO_4	15627	mmm	4	28	6.4	0	152	1.8	3.0	0
Na_2SO_3	31816	$\bar{3}$	2	12	6.4	41	761	3.0	7.0	0
Ta_4SiTe_4	40207	mmm	4	36	0	0	860	11.6	9.6	0
KBS_2	79614	$\bar{3}$m	6	24	3.8	0	113	10.1	17.3	0
AlCaSi	155193	6	6	18	0	0	5	15.3	47.9	1.1
$NaPt_2Se_3$	78788	6mm	4	24	1.6	0	989	2.2	7.6	1.2
$BaAl_2Si_2$	249559	mmm	4	20	0	0	4	40.6	20.7	4.6
$BaGe_2S_5$	66868	m$\bar{3}$m	4/16	32/ 128	3.2	0	131	43.3	12.7	5.3/−2.3*
$RbPSe_3$	173419	32	6	30	2.0	0	8	57.6	15.3	5.7
$CsIn_3O_5$	23630	mmm	4	36	2.8	0	2017	1.2	6.0	6.8
$KAsSe_2$	65297	1	4	16	2.3	0	4909	40.9	34.2	8.0
CaAsPt	60828	4mm	6	18	0	0	10	7.4	4.0	9.0

$AlBiCl_6$	414261	2/m	4	32	5.0	0	23	14.3	7.6	13.0
Na_3SbO_3	23346	$\bar{4}$3m	4/8	28/56	4.1	0	4958	2.4	8.1	13.3/0.0*
Sb_2OS_2	12120	$\bar{1}$	8	40	1.8	1	172	38.0	16.1	18.6
Na_2AuSn_3	107556	6/mmm	4	24	0	0	2357	36.6	8.3	25.3
$SnGeS_3$	411241	2/m	4	20	1.9	0	4993	75.5	227.3	30.0
YPdGe	391466	mm2	6/12	18/36	0	0	680	21.6	9.9	32.9/0.0*
$Sr_2Pt_3In_4$	410703	$\bar{6}$m2	4	36	0	0	3575	83.5	140.0	36.6

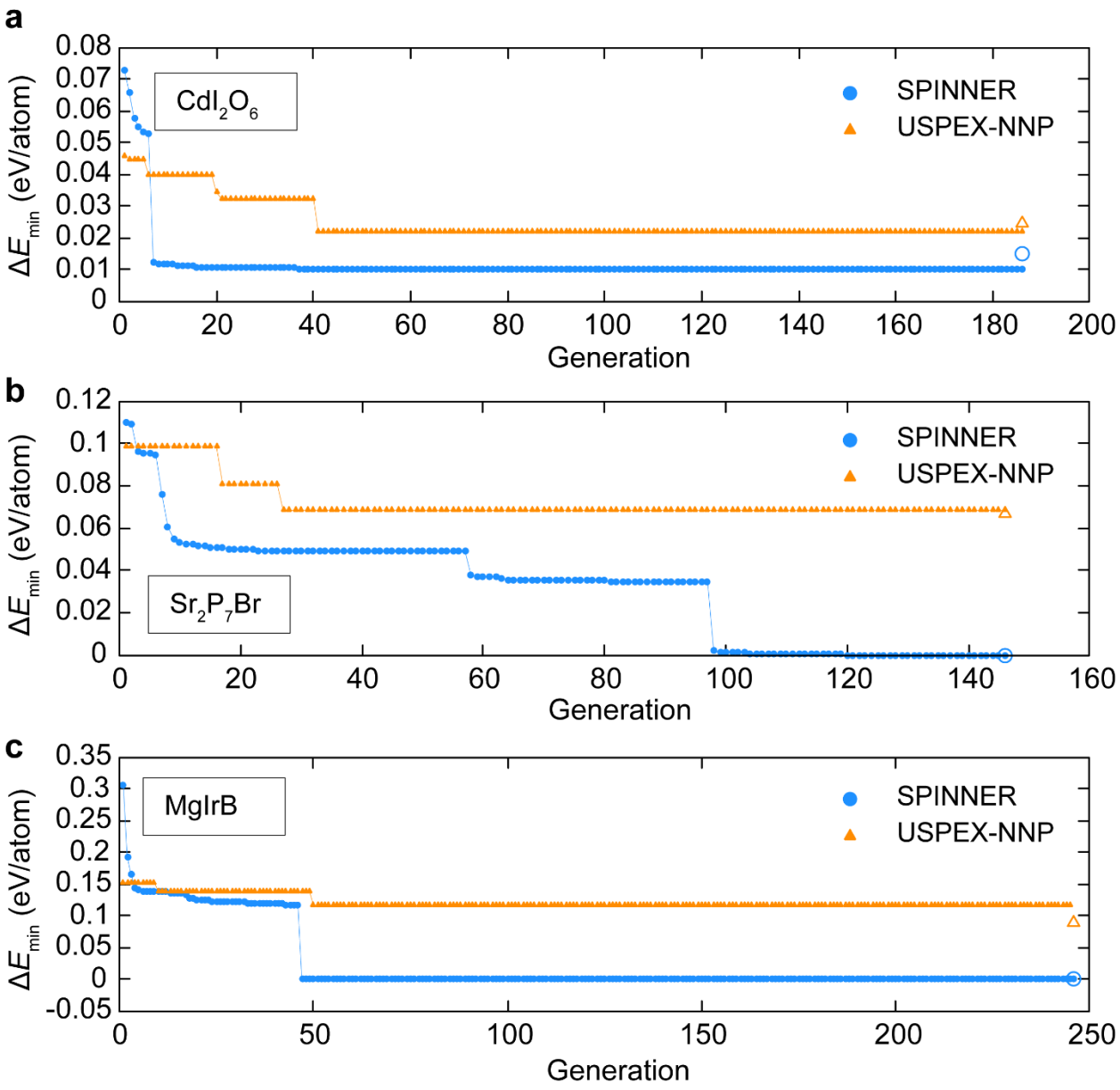

Supplementary Figure 3. Comparison of SPINNER with USPEX coupled with NNP for (a) CdI_2O_6, (b) Sr_2P_7Br, and (c) MgIrB. ΔE_{min} of filled points are calculated by NNP and the empty points are the lowest DFT energies of the structure candidates within 50 meV/atom.

Supplementary References

1. Kim, S. et al. A band-gap database for semiconducting inorganic materials calculated with hybrid functional. *Sci. Data* **7**, 387 (2020).

2. Jain, A. et al. The Materials Project: A materials genome approach to accelerating materials innovation. *APL Mater.* **1**, 011002 (2013).